

# Frequency estimation of ECG signals using FIR filter

**Sehleen Kaur**

M.Tech Research Scholar, ECED, Punjabi University, Patiala, Punjab, India

**Er. Amandeep Singh Bhandari**

Assistant Professor, ECED, Punjabi University, Patiala, Punjab, India

EMAIL: [kaursehleen@yahoo.com](mailto:kaursehleen@yahoo.com)

## Abstract

*The proposed system resembles a new family of dyadic wavelet tight frames based on two scaling purposes and four distinct wavelets. One pair of the four wavelets are designed to be offset from the other pair of wavelets so that the integer transforms of one wavelet pair fall midway between the integer translates of the other pair. Simultaneously, one pair of wavelets are designed to be approximate Hilbert transforms of the other pair of wavelets so that two complex (approximately analytic) wavelets can be formed. Therefore, they can be used to implement complex and directional wavelet transforms. It develops a design procedure to obtain finite impulse response (FIR) filters that satisfy the numerous constraints imposed. This design procedure employs a fractional-delay all pass filter, spectral factorization, and filter bank completion. The simulation results show considerable performance enhancements with high degree of smoothness.*

## 1. Introduction

ECG of a patient is observed visually in time dominion. But examining the ECG curve visually is typically inadequate. Signal processing approaches are performed to observe the ECG curve correctly. Frequency domain approaches, spectrum approximation and filtering are necessary to examine the ECG curve.

Circumstances such as movement of the patient, breathing and interaction between the electrodes and the skin cause baseline wandering of the ECG signal. Baseline wandering can mask some important features of the ECG signal hence it is desirable to

remove this noise for proper analysis and display of the ECG signal. Exploratory the ECG signal only in time domain is inadequate. Frequency domain ECG signal processing approaches are essential to observe the ECG spectra. Suppression of unwanted frequencies is necessary and it is mandatory to examine the ECG correctly. There are various filters to remove the baseline wandering noise. These are finite impulse response (FIR), infinite impulse response (IIR), adaptive and spline interpolation filters. This study contains an investigation of these methods, implementation and confirmation of each technique for offline applications. The offline filters with best performances are then designated and used in online applications [1].

## 2. Digital Filter Order, Step-Size and Coefficients

The design of digital filter involves decisive the order of filter and the values of coefficients in the representation of dissimilar equation.[2] The order, step-size and coefficient are essential to define performance of a digital filter, which are described below[3]:

### a. Order of a Digital Filter

The filter order defines the maximum exponents in the numerator or denominator ofz-transform equation of digital filter and also articulated as the number of previous inputs which are used to calculate the current output.The order of the digital filter is significant for its performance. If the filter order is larger, then better frequency magnitude response performance of the filter can be attained.

In FIR filters there is no denominator in its transfer function so it is often equal to the taps. In IIR filters it is equal to number of delay elements in filter structure. Different filter's orders are describes as [4]

### b. Zero-Order Filter

The zero-order filter is labelled as the current output  $y_n$  depends only on its current input  $x_n$  and not on any previous input.[5]

$$y_n = x_n$$

### c. First-Order Filter

The first-order filter only use the previous input and the current input is not used, so the previous input ( $x_n - 1$ ) is obligatory to calculate  $y_n$ . [6]

$$y_n = x_n - 1$$

### d. Second-Order Filter

The second-order filter calculate the current output  $y_n$ , two previous inputs ( $x_n - 1$  and  $x_n - 2$ ) are required; this is therefore called a second-order filter. [7]

$$y_n = (x_n + x_n - 1 + x_n - 2)/3$$

### e. Step-Size of a Digital Filter

Step-Size is necessary for the use of LMS algorithm, which can be determine by the cross-correlation among the reference and primary signals. The step-size depend of the Eigen value, if the Eigen value is maximum then the step size for convergence will also be maximum. The rate of convergence is proportional to the step-size and the minimum Eigen value, which is shown in the following equation:[8]

$$1/\tau \approx 2\mu\lambda_{min}$$

In the equation above,  $\mu$  is the step-size,  $\lambda_{min}$  is the minimum Eigen value, and  $\tau$  is the overall time-constant.[7]

## 3. Discrete Wavelet Transform

Resolution has been normally referred as an important feature of an image. Images are being managed in order to obtain more improved resolution. One of the generally used methods for image resolution improvement is Interpolation. Interpolation has been broadly used in many image processing applications such as facial rebuilding, various description coding [6], and fabulous resolution. There are three well identified interpolation methods, namely adjacent neighbor interpolation, bilinear interpolation, and bi-cubic interpolation. Image resolution improvement in the wavelet domain is a relatively new research topic and in recent times many new algorithms have been planned [4]. Discrete wavelet transform (DWT) is one of the recent wavelet transforms used in image processing.

The CWT (Continuous Wavelet Transform) performs multi resolution exploration by reduction and dilatation of the wavelet functions. The discrete wavelet transform uses filter banks for the building of the multi resolution time-frequency plane.[9] The DWT uses multi resolution filter banks and distinctive wavelet filters for the examination and reconstruction of signals.

## 4. ECG Denoising Using Wavelet Transform

In this proposed method, the corrupted ECG signal  $x(n)$  is denoised by taking the DWT of raw and noisy ECG signal. A family of the mother wavelet is available having the energy spectrum concentrated around the low frequencies like the ECG signal as well as better resembling the QRS complex of the ECG signal. We have used symlet wavelet, which resembles the ECG wave.

## 5. The Window Based FIR Filter Design

In this method, we start with the desired frequency response specification  $H_d(\omega)$  and the corresponding unit sample response  $h_d(n)$  is determined using inverse Fourier transform. The relation between  $H_d(\omega)$  and  $h_d(n)$  is as follows:

$$H_d(\omega) = \sum_{i=0}^{\infty} h_d(n)e^{-j\omega n}$$

$$H(\omega) = \sum_{i=0}^{\infty} h(n)e^{-j\omega n}$$

Where, the impulse response is given by,

$$h_d(n) = \int_{-\pi}^{\pi} H_d(\omega)e^{j\omega n} d\omega$$

The impulse response  $h_d(n)$  is of infinite duration. So, it is truncated at some point, say  $n = M - 1$  to yield an FIR filter of length  $M$  (i.e. 0 to  $M - 1$ ). This truncation of  $h_d(n)$  to length  $M - 1$  is done by multiplying  $h_d(n)$  with a window. Here the design is explained by considering the “rectangular window”, defined as

$$w(n) = \begin{cases} 1 & n = 0, 1, 2, \dots, M - 1 \\ 0 & \text{otherwise} \end{cases}$$

Thus, the impulse response of the FIR filter becomes

$$h(n) = h_d(n)w(n) = \begin{cases} h_d(n) & n = 0, 1, 2, \dots, M - 1 \\ 0 & \text{otherwise} \end{cases}$$

Now, the multiplication of the window function  $w(n)$  with  $h_d(n)$  is equivalent to convolution of  $H_d(\omega)$  with  $W(\omega)$ , where  $W(\omega)$  is the frequency domain representation (Fourier transform) of the window function i.e.

$$W(\omega) = \sum_{i=0}^{\infty} w(n)e^{-j\omega n}$$

Thus, the convolution of  $H_d(\omega)$  with  $W(\omega)$  yields the frequency response of the truncated FIR Filter  $H(\omega)$ .

$$H(\omega) = \frac{1}{2\pi} \int_{-\pi}^{\pi} H_d(v)W(n)e^{-j\omega n} d\omega$$

The frequency response can also be obtained by Fourier transform of  $h(n)$ , given in the following relation,

But direct truncation of the Fourier series  $h_d(n)$  to  $M$  terms to obtain  $h(n)$  is known to introduce ripples in the frequency response characteristic  $H(\omega)$ . It is due to the non-uniform convergence of the Fourier series at a discontinuity. The Oscillatory behaviour near the band edge of the filter is called *Gibbs phenomenon*. Thus, the frequency response obtained contains ripples in the frequency domain.

In order to reduce the ripples,  $h_d(n)$  is multiplied with a window function that contains a taper and decays toward zero gradually instead of abruptly as it occurs in a rectangular window. As multiplication of sequences  $h_d(n)$  and  $w(n)$  in time domain is equivalent to convolution of  $H_d(\omega)$  and  $W(\omega)$  in the frequency domain, it has the effect of smoothing  $H_d(\omega)$ .

## 6. Implementation

The  $z$ -transform of  $h_i(n)$  is denoted by  $H_i(z)$

$$H_i(z) = ZT\{h_i(n)\} = \sum_n h_i(n)z^{-n}$$

And  $G_i(z)$  is similarly defined. It is assumed that all filter coefficients  $h_i(n)g_i(n)$  are real valued. The frequency response  $H_i(e^{j\omega})$  is given by

$$H_i(e^{j\omega}) = DTFT\{h_i(n)\} = \sum_n h_i(n)e^{-j\omega n}$$

And,  $G_i(e^{j\omega})$  is similarly defined. The filters  $h_i(n)$  and  $g_i(n)$  should satisfy the perfect reconstruction (PR) conditions. From basic multirate identities, the PR conditions are the following:

$$\sum_{i=0}^2 H_i(z) H_i\left(\frac{1}{z}\right) = 2$$

$$\sum_{i=0}^2 H_i(z) H_i\left(-\frac{1}{z}\right) = 0$$

$$\sum_{i=0}^2 G_i(z) G_i\left(\frac{1}{z}\right) = 2$$

$$\sum_{i=0}^2 G_i(z) G_i\left(-\frac{1}{z}\right) = 0$$

The scaling and wavelet functions are defined implicitly through the dilation and wavelet equations, given by,

$$\phi_h(t) = \sqrt{2} \sum_n h_0(n) \phi_h(2t - n)$$

$$\psi_{h,1}(t) = \sqrt{2} \sum_n h_1(n) \phi_h(2t - n)$$

$$\psi_{h,2}(t) = \sqrt{2} \sum_n h_2(n) \phi_h(2t - n)$$

Where  $\phi_g(t)$  and  $\psi_{g,i}(t)$  are defined similarly. The Fourier transforms of the scaling functions and wavelets will be denoted as,

$$\Phi_h(\omega) = \mathcal{F}\{\phi_h(t)\}, \Phi_g(\omega) = \mathcal{F}\{\phi_g(t)\}$$

$$\Psi_{h,i}(\omega) = \mathcal{F}\{\psi_{h,i}(t)\}, \Psi_{g,i}(\omega) = \mathcal{F}\{\psi_{g,i}(t)\}$$

The Hilbert transform of a function  $f(t)$  will be denoted as  $\mathcal{H}\{f(t)\}$ . Following the work by Kingsbury, we want the wavelets to form Hilbert transform pairs,

$$\psi_{g,1}(t) = \mathcal{H}\{\psi_{h,1}(t)\}$$

$$\psi_{g,2}(t) = \mathcal{H}\{\psi_{h,2}(t)\}$$

Recalling the definition of the Hilbert transform, this means that,

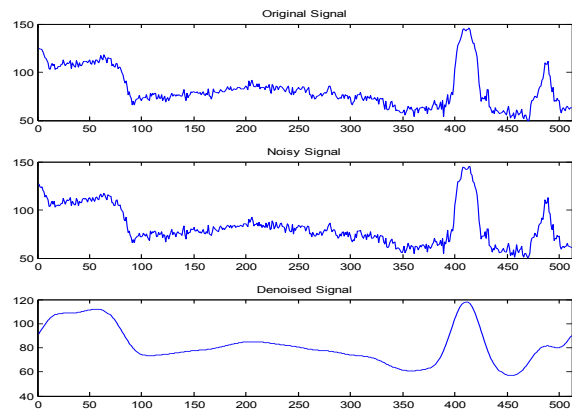
$$\Psi_{g,i}(\omega) = \begin{cases} -j\Psi_{h,i}(\omega), & \omega > 0 \\ j\Psi_{h,i}(\omega), & \omega < 0 \end{cases}$$

## 7. Results

### a. Test Case #1

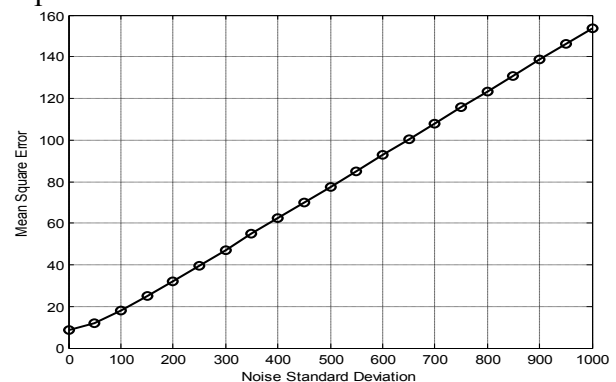
The test case considers a general one dimension signal called the *original signal* which is used to create a new signal called *noisy signal* by adding AWGN and Rayleigh noise of known variance. The *noisy signal* is denoised using the proposed filter to generate the *denoised signal*.

Fig. 1.1 shows the results of the complete process. In this case only AWGN noise was added to the *original signal* with zero mean and standard deviation equal to unity. The computed threshold for the denoised signal was  $2.0058e+13$  and the mean square error was 8.5436.



**Figure 1.1:** Test Case #1 (AWGN only)

Fig. 1.2 shows the mean square error for various values of noise standard deviation with AWGN noise only. Noise Mean is zero in each case. As shown the relation is linear as expected.



**Figure 1.2:** Test Case #1 (AWGN only) (MSE vs. Standard Deviation)

Now, we will create the *noisy signal* by adding AWGN and Rayleigh noise of known variance.

Fig. 1.3 shows the results of the complete process. In this case AWGN and Rayleigh noise were added to the *original signal* with zero mean and standard deviation equal to unity. The computed threshold for the denoised signal was  $1.0029e+13$  and the mean square error was 16.2801.

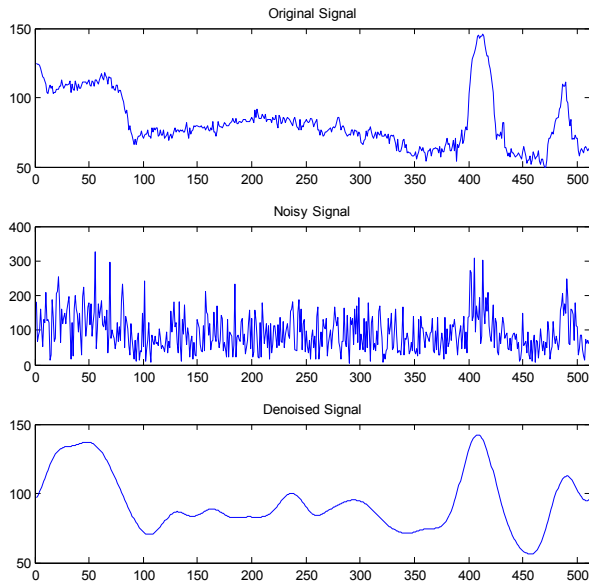


**Figure 1.3:** Test Case #1 (AWGN + Rayleigh)

Fig. 1.4 shows the mean square error for various values of noise standard deviation with AWGN + Rayleigh. Noise Mean is zero in each case. As shown the relation is linear as expected.

As seen from both the results obtained (with AWGN only, and AWGN + Rayleigh) we can see that the increase in the noise level will increase the mean square error. The mean square error is calculated between the *original* and the *denoised* signal.

As the Rayleigh noise would degrade the *original signal* more than AWGN alone, the mean square error would be more in former case. The obtained results illustrate this fact.

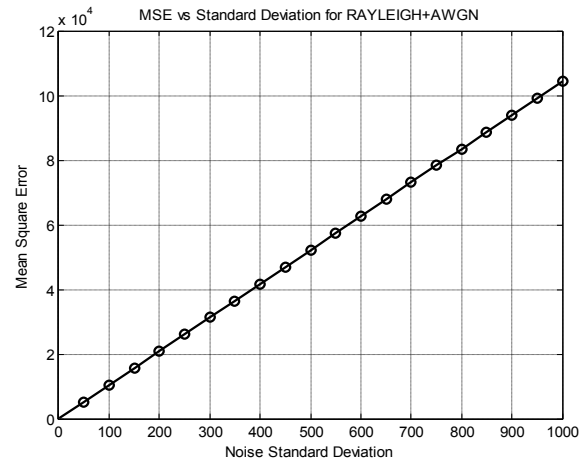
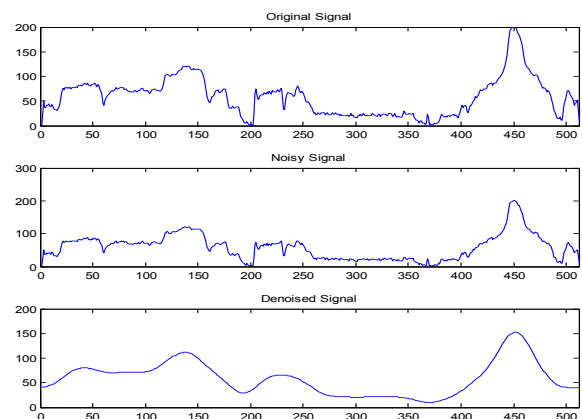


**Figure 1.4:** Test Case #1 (AWGN + Rayleigh) (MSE vs. Standard Deviation)

**b. Test Case #2**

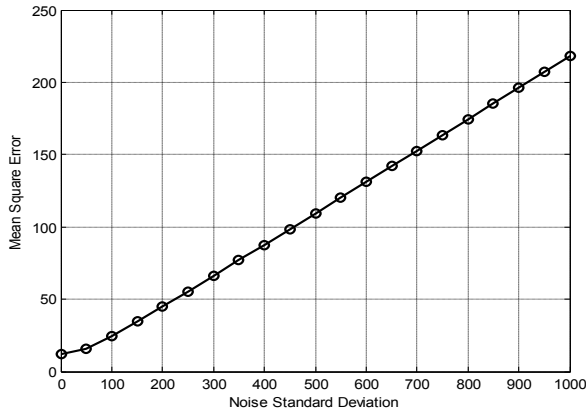
The test case considers another general one dimension signal *original signal* used to create a *noisy signal* by adding AWGN and Rayleigh noise of known variance. The *noisy signal* is denoised using the proposed filter to generate the *denoised signal*.

Fig. 1.4 shows the results of the complete process. In this case only AWGN noise was added to the *original signal* with zero mean and standard deviation equal to unity. The computed threshold for the denoised signal was  $1.6715e+13$  and the mean square error was 12.3609. Fig. 1.5 shows the mean square error for various values of noise standard deviation with AWGN noise only. Noise Mean is zero in each case. As shown the relation is linear as expected.



**Figure 1.5:** Test Case #2 (AWGN only)





**Figure 1.6:** Test Case #2 (AWGN only) (MSE vs. Standard Deviation)

Now, we will create the *noisy signal* by adding AWGN and Rayleigh noise of known variance. Fig. 1.7 shows the results of the complete process. In this case AWGN and Rayleigh noise were added to the *original signal* with zero mean and standard deviation equal to unity. The computed threshold for the denoised signal was  $1.1144e+13$  and the mean square error was 18.2465.

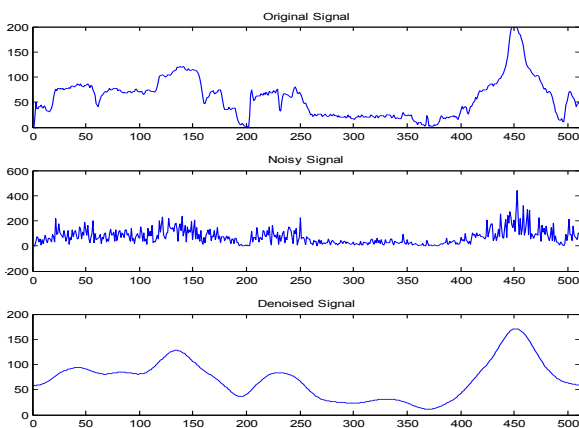


**Figure 1.7:** Test Case #2 (AWGN + Rayleigh)

Fig. 1.8 shows the mean square error for various values of noise standard deviation with AWGN + Rayleigh. Noise Mean is zero in each case. As shown the relation is linear as expected.

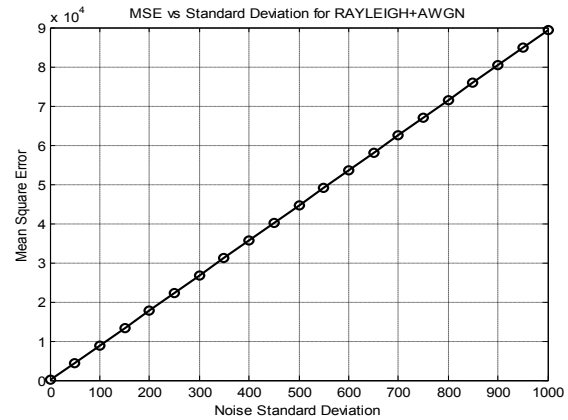


**Figure 1.8:** Test Case #2 (AWGN + Rayleigh) (MSE vs. Standard Deviation)

As seen from both the results obtained (with AWGN only, and AWGN + Rayleigh) we can see that the increase in the noise level will increase the mean square error. The mean square error is calculated between the *original* and the *denoised* signal. As the Rayleigh noise would degrade the *original signal* more than AWGN alone, the mean square error would be more in former case. The obtained results illustrate this fact.

### c. Test Case #3

The test case considers a *noisy ECG signal* generated using in-built Matlab data file (*noisyecg.mat*). This in-built *noisy ECG signal* has a baseline shift and therefore does not represent the true amplitude. In order to remove the trend, a low order polynomial is fitted to the *noisy ECG signal* and that polynomial is then used to de-trend it. This doesn't remove any noise, but only remove the base line wander. As the noise is already added, so there is no need to re-add noise to this signal. The *noisy ECG signal* is further denoised using the proposed filter to generate the *denoised signal*.

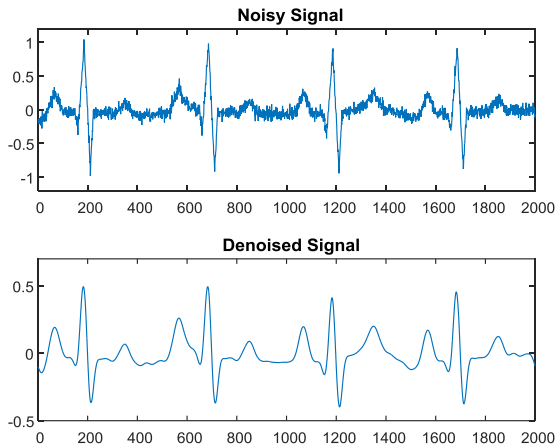


**Figure 1.9: Test Case #3**

Fig. 1.9 shows the results of the complete process. The computed threshold for the denoised signal was  $2.8528e+15$  and the mean square error was 0.1030.

## 8. Comparison

A smaller MSE implies a shorter transient duration. The notch filter given in [10] with time varying radius achieves an MSE of 0.12 while the traditional notch filter obtains an MSE of 0.2. The filter proposed in this work achieves an MSE of 0.10. Hence, it is clear that the proposed notch filter is effective in reducing transient response compared to traditional filters. It is also worth noting that higher order filters achieve lower MSE at the cost of increase in processing power and complexity.

**Table 1.1: MSE Comparison**

	Filter [10]	Filter[11]	Traditional Filter	Proposed Filter
<b>MSE</b>	<b>0.12</b>	<b>0.35</b>	<b>0.2</b>	<b>0.10</b>

**Conclusion** ECG is a measure of electrical activity of the heart over time. The signal is measured by electrodes attached to the skin and is sensitive to disturbances such as power source interference and noises due to movement artifacts. ECG of a patient is observed visually in time dominion. But examining the ECG curve visually is typically

inadequate. Signal processing approaches are performed to observe the ECG curve correctly. Frequency domain approaches, spectrum approximation and filtering are necessary to examine the ECG curve.

This work used a wavelet based window FIR filter that combined the discrete wavelet transform and two level FIR filter, each of which has its own characteristics and benefits. The proposed system resembles a new family of dyadic wavelet tight frames based on two scaling purposes and four distinct wavelets. One pair of the four wavelets are designed to be offset from the other pair of wavelets so that the integer transforms of one wavelet pair fall midway between the integer translates of the other pair.

Simultaneously, one pair of wavelets are designed to be approximate Hilbert transforms of the other pair of wavelets so that two complex (approximately analytic) wavelets can be formed. Therefore, they can be used to implement complex and directional wavelet transforms. This work developed a design procedure to obtain finite impulse response (FIR) filters that satisfy the numerous constraints imposed. This design procedure employed a fractional-delay all pass filter, spectral factorization, and filter bank completion. The simulation results show considerable performance enhancements with high degree of smoothness. Comparison based on mean square error, with previous work shows significant improvement in the noise reduction using proposed filter.

## References

- [1] H. B. Barlow, "Possible principles underlying the transformation of sensory messages," in *Sensory Communication*, 1961.
- [2] O. Sayadi and M. B. Shamsollahi, "Multiadaptive bionic wavelet transform: Application to ECG denoising and baseline wandering reduction," *EURASIP Journal on Advances in Signal*

*Processing*, vol. 2007, no. 1, p. 041274, 2007.

- [3] G. Clifford, L. Tarassenko and N. Townsend, "One-pass training of optimal architecture auto-associative neural network for detecting ectopic beats," *Electronics Letters*, vol. 37, no. 18, pp. 1126-1127, 2001.
- [4] P. C. Teo and D. J. Heeger, "Perceptual image distortion," in *in Proc. SPIE*, 1994.
- [5] R. Mark, P. Schluter, G. Moody, P. Devlin and D. Chernoff, "An annotated ECG database for evaluating arrhythmia detectors," in *IEEE Transactions on Biomedical Engineering*, 1982.
- [6] N. Damera-Venkata, T. Kite, W. Geisler, B. Evans and A. Bovik, "Image quality assessment based on a degradation model," *Image Processing, IEEE Transactions on*, vol. 9, no. 4, pp. 636-650, Apr 2000.
- [7] D. L. Donoho, "De-noising by soft-thresholding," *Information Theory, IEEE Transactions on*, vol. 41, no. 3, pp. 613-627, 1995.
- [8] S. Jagtap, M. Chavan, R. Wagvekar and M. Uplane, "Application of the digital filter for noise reduction in electrocardiogram," *Journal of Instrumentation*, vol. 40, no. 2, pp. 83-86, 2010.
- [9] G. Strang and T. Nguyen, *Wavelets and Filter Banks*, Wellesley College, 1996.
- [10] R. Rajagopalan and A. Dahlstrom, "A Pole Radius Varying Notch Filter with Transient Suppression for Electrocardiogram," *International Journal of Medical, Health, Pharmaceutical and Biomedical Engineering*, vol. 8, no. 3, 2014.
- [11] L. Tan, J. Jiang and L. Wang, "Pole-radius-varying IIR notch filter with transient suppression," *Instrumentation and Measurement, IEEE Transactions on*, vol. 61, no. 6, pp. 1684-1691, 2012.